Hindawi Publishing Corporation
International Journal of Polymer Science
Volume 2016, Article ID 2862738, 8 pages
http://dx.doi.org/10.1155/2016/2862738

Research Article

Porous Lactose-Modified Chitosan Scaffold for Liver Tissue Engineering: Influence of Galactose Moieties on Cell Attachment and Mechanical Stability

Birong Wang,[1] Qinggang Hu,[2] Tao Wan,[3] Fengxiao Yang,[3,4] Le Cui,[1] Shaobo Hu,[2] Bo Gong,[5] Min Li,[2] and Qi Chang Zheng[2]

[1]*Department of Breast and Thyroid Surgery, Puai Hospital, Wuhan 430035, China*
[2]*Department of Hepatobiliary Surgery, Union Hospital, Tongji Medical College, Huazhong University of Science and Technology, Wuhan 430022, China*
[3]*Biomedical Materials and Engineering Center, Wuhan University of Technology, Wuhan 430070, China*
[4]*Xiamen Niell Electronics Co., Ltd., Xiamen 361000, China*
[5]*Department of General Surgery, Xiantao Hospital of Traditional Chinese Medicine, Xiantao 433000, China*

Correspondence should be addressed to Min Li; liminmed@hust.edu.cn and Qi Chang Zheng; qc_zheng@hust.edu.cn

Received 8 November 2015; Revised 3 January 2016; Accepted 12 January 2016

Academic Editor: Vitor Sencadas

Galactosylated chitosan (CTS) has been widely applied in liver tissue engineering as scaffold. However, the influence of degree of substitution (DS) of galactose moieties on cell attachment and mechanical stability is not clear. In this study, we synthesized the lactose-modified chitosan (Lact-CTS) with various DS of galactose moieties by Schiff base reaction and reducing action of $NaBH_4$, characterized by FTIR. The DS of Lact-CTS-1, Lact-CTS-2, and Lact-CTS-3 was 19.66%, 48.62%, and 66.21% through the method of potentiometric titration. The cell attachment of hepatocytes on the CTS and Lact-CTS films was enhanced accompanied with the increase of galactose moieties on CTS chain because of the galactose ligand-receptor recognition; however, the mechanical stability of Lact-CTS-3 was reduced contributing to the extravagant hydrophilicity, which was proved using the sessile drop method. Then, the three-dimensional Lact-CTS scaffolds were fabricated by freezing-drying technique. The SEM images revealed the homogeneous pore bearing the favorable connectivity and the pore sizes of scaffolds with majority of 100 μm; however, the extract solution of Lact-CTS-3 scaffold significantly damaged red blood cells by hemolysis assay, indicating that exorbitant DS of Lact-CTS-3 decreased the mechanical stability and increased the toxicity. To sum up, the Lact-CTS-2 with 48.62% of galactose moieties could facilitate the cell attachment and possess great biocompatibility and mechanical stability, indicating that Lact-CTS-2 was a promising material for liver tissue engineering.

1. Introduction

Serving as an interdisciplinary field in biomedical engineering, liver tissue engineering aims to regenerate new living tissue for replacing diseased or damaged tissues/organs in recent years [1]. The three-dimensional scaffold, as one of the three essential factors of tissue engineering, is playing an extremely important role as adhesive substrate and in connective tissue framework and payload and storage of growth factors [2, 3]. Therefore, development of new class artificial scaffold is an imperative task to guide cell attachment, survival, cell morphological changes, proliferation, and differentiation for liver tissue engineering.

The constituents of extracellular matrix (ECM) materials are one of the most important key factors to determine the properties of tissue scaffold. As a natural biomaterial with its essential advantage in biodegradation, biocompatibility, and nonimmunoreaction, chitosan (CTS) is an ideal ECM material for three-dimensional scaffold [4–6]. Thus, the CTS and its derivatives are widely applied in tissue engineering

[7]. Additionally, the micromorphology and structure could impact the properties of scaffold and the cells growth as well. The porous structure and favorable pore connectivity of scaffolds are beneficial to the penetration of nutrients and the normal cell metabolism. Researches indicated that sufficient space and surface area of scaffold were able to offer the suitable surroundings for the cell adhesion, proliferation, and differentiation [8]. Among the methods of scaffold fabrication, the freezing-drying technique was recommended to produce the well-structured scaffolds with high porosity and appropriate aperture determined by the freezing degree [9]. In recent years, the three-dimensional CTS sponges with high porosity and mechanical stability were fabricated by freezing-drying technique and could maintain liver-specific functions [3, 10, 11], indicating that the CTS scaffolds could be promising as novel hepatocytes substrates for liver tissue engineering, such as bioartificial liver-assist devices and liver regeneration.

Besides, because of its abundant hydroxyl and amino groups, CTS can be easily modified with specific ligands [12–15], which provides reaction site to link some ligand of liver parenchyma to improve the affinity between seed cells and tissue scaffold. These ligands can induce the seed cells to attach the scaffold and accelerate the recovery of cellular functions. It is confirmed that asialoglycoprotein receptors (ASGP-R) are overexpressed on the surface of hepatocytes and selectively bind to galactose ligands [2, 5, 16, 17]. Recently, many researches demonstrated that the interaction between ASGP-R and galactose ligand can facilitate the attachment and aggregates formation of hepatocytes and enhance maintenance of liver-specific functions [2]. Therefore, Park et al. covalently coupled CTS with galactose moieties, which indicated that hepatocytes adhered to two-dimensional galactosylated CTS film with spreading shapes [9]. Feng et al. fabricated three-dimensional galactosylated CTS scaffold with high cell attachment and liver-specific function maintenance in terms of albumin synthesis and urea metabolism [2]. However, so far, it is not clear whether the degree of substitution (DS) of galactose moieties in the backbone of CTS affects the cell attachment and mechanical property of the scaffold.

Herein, we investigate the influence of galactose moieties in CTS scaffold on the cell attachment, mechanical properties, and biocompatibility. In this study, the lactose-modified chitosan (Lact-CTS) was successfully synthesized through Schiff base reaction between the glucose group of lactose and amino group of CTS under the reducing action of $NaBH_4$, and then the porous scaffolds were prepared by freezing-drying technique. The chemical structures of the products were characterized by Fourier transform infrared spectrometry (FTIR), the physicochemical properties were measured by potentiometric titration and other methods, and the morphology of scaffolds was observed using scanning electron microscope (SEM). Moreover, the hepatocytes attachment on Lact-CTS films was monitored under phase contrast microscope and the hemolysis assay and cell growth on Lact-CTS scaffolds were performed to evaluate the biocompatibility of Lact-CTS for liver tissue engineering.

2. Materials and Methods

2.1. Materials. Chitosan (MW: 300 kDa, degree of deacetylation: 84%) was purchased from Yuhuan Ocean Biochemical (Zhejiang, China). Lactose and $NaBH_4$ were purchased from Sinopharm Chemical Reagent Co., Ltd. (Shanghai, China). Other chemicals were of analytical reagent grade. Normal liver cell LO2 was obtained from the Cell Bank of the Chinese Academy of Sciences (Shanghai, China). RPMI 1640 medium and fetal bovine serum (FBS) were purchased from Hyclone Labs. (Logan, USA). Trypsin and penicillin-streptomycin mixtures were bought from Sigma-Aldrich (St. Louis, USA).

2.2. Synthesis of Lact-CTS. Coupling of lactose with chitosan was carried out by the reducing agent as described previously [18]. Briefly, 8.0 g of lactose was added to 50 mL of the chitosan solution (1.5 wt% in 1% acetic acid solution), under magnetic stirring for 1 h at room temperature. Then, 0.2, 0.6, and 1.6 g of $NaBH_4$ were put into the mixture, respectively. After reaction for 25 h at room temperature, the product was dialyzed against distilled water for 2 days, followed by lyophilization to obtain the final products Lact-CTS-1, Lact-CTS-2, and Lact-CTS-3, respectively.

2.3. FTIR. FTIR spectra were recorded using FTIR spectrometer (Thermo Nicolet Corp., Madison, USA). Dried samples were ground with KBr powder and compressed into pellets for FTIR examination.

2.4. Measurement of DS. The DS of lactose in Lact-CTS was calculated by potentiometric titration method [19]. Briefly, 0.1 g of Lact-CTS-1, 0.1 g of Lact-CTS-2, and 0.1 g of Lact-CTS-3 powder were dissolved in solvent of 1% hydrochloric acid at the concentrations of 0.3% (wt/v), respectively. Then, as the titrating solution, 0.1 mol/L of NaOH was added to the previous acid solution to measure the different pH value of the solution under different volume of standard caustic soda solution. The DS was evaluated as follows:

$$\mathrm{DS} = 1 - \frac{\Delta V \times C_{\mathrm{NaOH}} \times 16}{m \times 0.0994} \times 100\%. \quad (1)$$

In the formula, the consumption of NaOH (ΔV, mL) was obtained by the changed volume in the process of two mutations. C_{NaOH} (mol/mL) stands for the concentration of NaOH, m represents the constant weight of sample, and constants 16 and 0.0994 (g) are the formula weight of amino group and the theoretical amount of amino group.

2.5. Analysis of Contact Angle. The contact angle of samples was determined by using the sessile drop method with the contact angle instrument JC2000A (Shanghai Advanced Photoelectric Technology Co., Ltd., China) at room temperature. The CTS, Lact-CTS-1, Lact-CTS-2, and Lact-CTS-3 films were prepared in glass slips and dried naturally at room temperature, respectively. Subsequently, 5 μL distilled water was dropped to the surface of the films, and the bead modality of dripping was measured in 10 seconds.

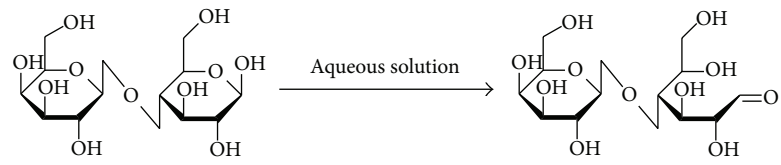

Figure 1: The chemical structure of lactose in aqueous solution.

2.6. Cell Culture and Attachment on the Lact-CTS Films. LO2 cells were cultured in the RPMI 1640 medium supplemented with 10% FBS, 100 U/mL penicillin, and 100 μg/mL streptomycin at 37°C in a humidified incubator with 5% CO_2 until reaching 80–90% confluence. The CTS, Lact-CTS-1, Lact-CTS-2, and Lact-CTS-3 films were also prepared in glass slips and dried naturally at room temperature, respectively. And then the films were sterilized by UV irradiation. The cells were seeded onto CTS and Lact-CTS films in 96-well plate and the morphology changes of adhered cells were observed using an Olympus phase contrast microscope (Olympus, Japan).

2.7. Fabrication of Lact-CTS Porous Scaffold. The Lact-CTS solution was prepared by dissolving the powder in solvent of 1% acetic acid at the concentration of 3.0 wt%. Subsequently, 0.25% glutaraldehyde solution was added to the acid solution [20]. The mixture was added as 0.5 mL per well to a 96-well microplate and precooled for 4 h at 4°C; then the Lact-CTS scaffolds were prepared by lyophilizing methods at −20°C. Finally, the scaffolds in reserve were operated by the secondary freeze drying.

2.8. Characterization of Porous Lact-CTS Scaffolds. The morphology of Lact-CTS scaffold was observed using JSM 5610LV SEM (JEOL, Japan). Cross sections were mounted onto an aluminum stub and coated with gold/palladium using JEOL JFC-1l0E Ion Sputter and the average pore size of the scaffolds was determined using image analysis system.

The porosity [21] and swelling ratio [22] of Lact-CTS scaffold were measured according to the literature with minor modification, respectively.

2.9. Hemolysis Assay. The scaffold extract solution was prepared through infiltrating the dried Lact-CTS-1, Lact-CTS-2, and Lact-CTS-3 scaffolds into 1x PBS (wt/v, 0.05 and 0.1 g/mL) at 37 ± 1°C for 24 h. Ethylenediaminetetraacetic acid- (EDTA-) stabilized human blood samples were freshly collected from Union Hospital (Wuhan, China) according to the literature with minor modification [23, 24]. The research was approved by the Institutional Review Board of Tongji Medical College of Huazhong University of Science and Technology. The patients provided informed written consent before blood sampling. In brief, 2.5 mL of blood sample was mixed with 5 mL of 1x PBS (pH = 7.2) and red blood cells (RBCs) were isolated from serum by centrifugation at 10,016 g for 10 min. Then, RBCs were rinsed five times with 5 mL of PBS solution and the purified blood was diluted to 25 mL with PBS. 40 μL diluted blood suspension was added to 160 μL scaffold extract solution and mixed by vortexing. Herein, blood incubation with PBS and blood incubation with DI water were used as the negative and positive controls, respectively. All sample tubes were kept in static condition at 37°C for 3 hours. Finally, the mixtures were centrifuged at 10,016 g for 5 min and 100 μL supernatant of all samples was transferred to a 96-well plate. The absorbance values were measured at 570 nm by using a microplate reader (Thermo Electron, Finland).

2.10. Statistical Analysis. The data were expressed as mean ± standard deviation (SD) from three independent experiments. The analysis of variance was performed using Dunnett's test by PASW Statistics (SPSS Inc., Chicago, IL). A value of $P < 0.05$ was considered statistically significant.

3. Results and Discussion

3.1. Preparation and Characterization of Lact-CTS. The lactose is a disaccharide sugar composed of galactose and glucose groups. In aqueous solution, the glucose groups of lactose exhibit both hemiacetal hydroxyl of ring structure and carbonyl of chain structure illustrated in Figure 1, whereas galactose groups keep stable ring structure. Through the Schiff base reaction and the reducing action of $NaBH_4$, the chemical bond was formed between the carbonyl groups on lactose and the primary amines on CTS. As shown in Figure 2, the Lact-CTS was successfully synthesized.

The product was characterized by FTIR from satisfactory analysis data were obtained. The FTIR spectra of CTS, Lact-CTS-1, Lact-CTS-2, and Lact-CTS-3 were shown in Figure 3. The peak form and peak position of Lact-CTS-1, Lact-CTS-2, and Lact-CTS-3 were quite similar but not identical with CTS. The characteristic absorption peaks of CTS at 1650 and 1597 cm^{-1}, which were attributed to I and II amides, indicate the presence of abundant free amino groups in CTS molecules [3]. When comparing FTIR spectra of Lact-CTS with those of CTS, the characteristic absorption of amides in CTS weakened contributing to the chemical changes between the amino groups of CTS and the aldehyde groups of lactose and slightly shifted to 1641 cm^{-1} in Lact-CTS, representing the bond of Schiff base. These intermolecular conformational changes indicated that lactose was introduced into CTS chains.

3.2. Determination of DS. The DS of galactose moieties on CTS was measured by potentiometric titration method, based on the amount of the consumption of NaOH in the process

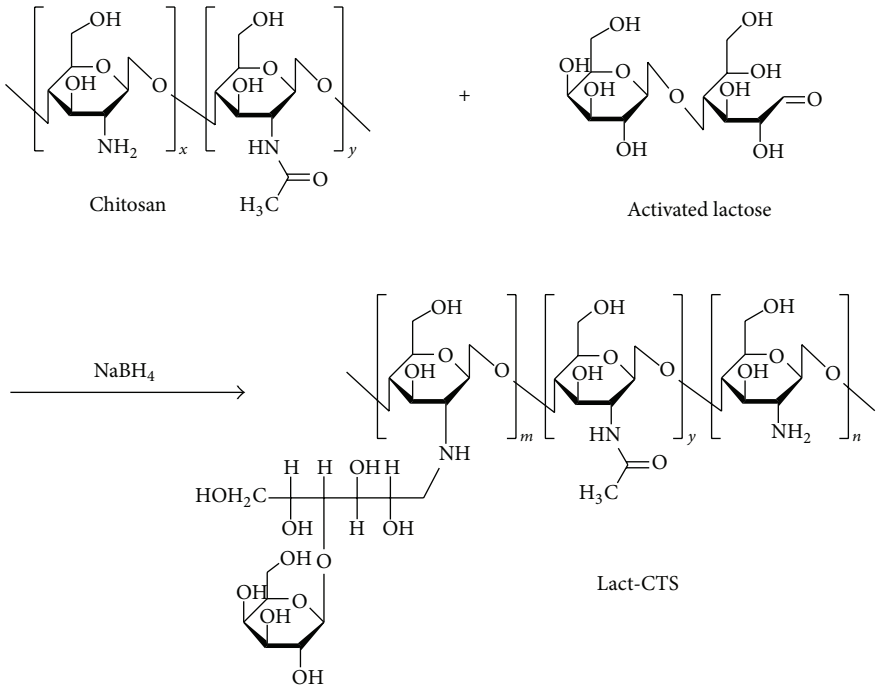

Figure 2: The scheme of Lact-CTS synthesis.

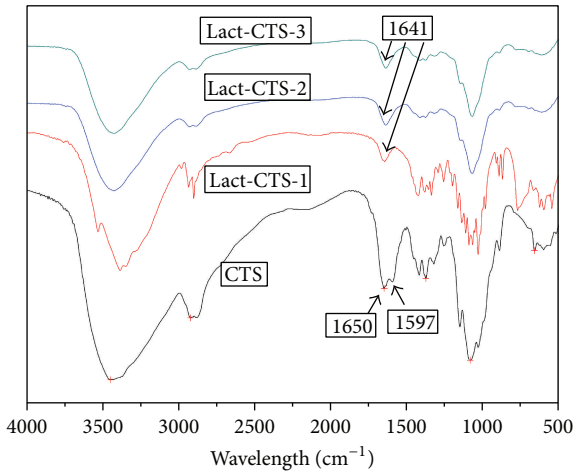

Figure 3: FTIR spectra of CTS, Lact-CTS-1, Lact-CTS-2, and Lact-CTS-3.

of the two mutations. Figures 4(a), 4(c), and 4(e) show the pH value titration curve of Lact-CTS-1, Lact-CTS-2, and Lact-CTS-3, respectively, exhibiting the notion that the pH value increased along with adding more NaOH solution. The first point of mutation appeared through the reaction of NaOH and the excess HCl on curve, presenting rapid rising of the pH value of solution. Among the two mutations, the consumption of NaOH was to be equivalent to the amount of the free amino groups on CTS backbone. Figures 4(b), 4(d), and 4(f) show the first-derivative curves of them, which were calculated through the consumption of NaOH in the process of the two mutations. According to the formula, the DS of Lact-CTS-1, Lact-CTS-2, and Lact-CTS-3 were figured out to be 19.66%, 48.62%, and 66.21%, respectively.

3.3. Analysis of Contact Angle. The contact angle of the products, reflecting the relative strength and surface hydrophilicity, was measured by the static sessile drop method. The lower contact angle suggests that the biomaterials possess better surface hydrophilicity for tissue engineering, which directly influences the adhesion and proliferation of living cells on the surface of materials [25]. As shown in Figure 5, the contact angle of CTS film was 83.9° and these of Lact-CTS-1 and Lact-CTS-2 were 69° and 40.4°, respectively, whereas the Lact-CTS-3 film had serious deformation as soon as it came into contact with the water drop. The phenomenon demonstrated that the hydrophilicity of films was dependent on the DS of galactose moieties on CTS chain; that is to say, the hydrophilicity of Lact-CTS was enhanced along with increasing the galactose moieties. On the other hand, the deformed Lact-CTS-3 was too hydrophilic to poor mechanical stability. All data indicated that Lact-CTS-2 exhibited the lowest contact angle providing the best hydrophilicity to benefit the cell growth, as well as favorable stability.

3.4. Galactose Moieties Induced Attachment of Hepatocytes on Films. The cell attachment between seed cells and artificial ECM can be facilitated through the galactose ligand-receptor recognition and maintain the liver-specific functions [26]. The specific interaction can activate the cell biological behaviors [27, 28]. We investigated the cell attachment on Lact-CTS films to assess influence of DS of galactose moieties on liver cells growth. The morphology of hepatocytes LO2 adhered to CTS, Lact-CTS-1, Lact-CTS-2, and Lact-CTS-3 films was

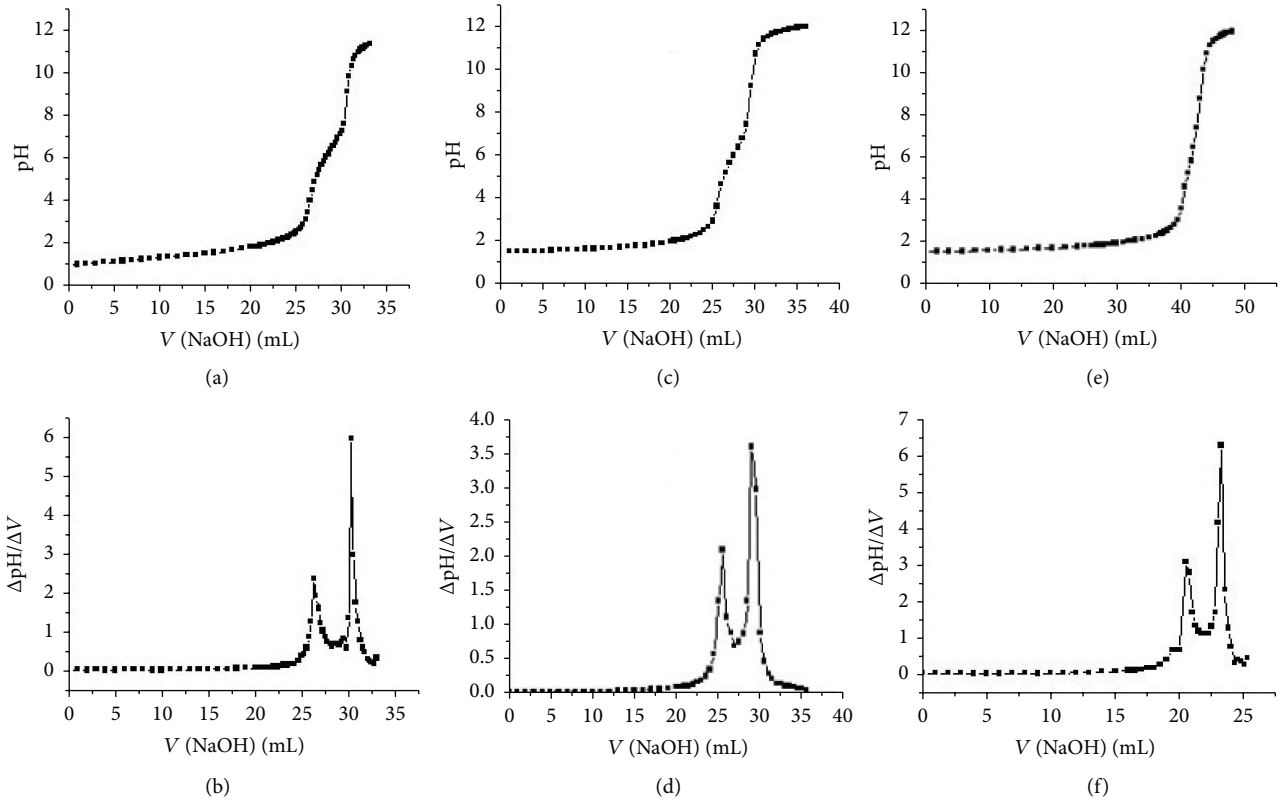

Figure 4: The DS of lactose in Lact-CTS by potentiometric titration method. The pH value titration curve of (a) Lact-CTS-1, (c) Lact-CTS-2, and (e) Lact-CTS-3. The first-derivative curves of (b) Lact-CTS-1, (d) Lact-CTS-2, and (f) Lact-CTS-3.

shown in Figure 6. The LO2 cells attached on various films were of round shapes after seeding for 30 min, whereas the partial cells on Lact-CTS-2 and Lact-CTS-3 films exhibited spheroid shapes comparing with CTS and Lact-CTS-1 films after 2 hours. After attachment for 6 hours, a majority of cells on Lact-CTS-2 and Lact-CTS-3 films recuperated spreading shapes, just about normal morphology. However, the cells on CTS and Lact-CTS-1 did not completely spread. The results suggest that the galactose moieties facilitate cells recovery of original morphology and biological behaviors.

3.5. Characterizations of Porous Lact-CTS Scaffolds. The Lact-CTS scaffold was fabricated by using the freezing-drying technique, which is a common method for preparation of tissue engineering scaffold. As shown in Figure 7, the three-dimensional Lact-CTS-2 scaffolds possessed uniform aperture and good interconnectivity. The microstructure morphology of the other three scaffolds was similar to that of Lact-CTS-2, so their images had not been shown. It is reported that the pore with a size of 100 μm is the most beneficial to liver cells reunion [29]. The pore size of Lact-CTS scaffolds ranges from 20 μm to 150 μm, including the majority of 100 μm.

The porosity and swelling ratio of scaffolds are important parameters for tissue engineering which determine the cell attachment, migration, proliferation, and so on [30]. As illustrated in Table 1, the high porosity of CTS, Lact-CTS-1, Lact-CTS-2, and Lact-CTS-3 scaffolds all was more than these of liver scaffolds reported in previous literature [11]. On the other hand, the four scaffolds had great swelling ratio property and the swelling ratio was enhanced accompanied with increasing the DS of galactose moieties.

Table 1: Porosity and swelling ratios of CTS and Lact-CTS scaffolds.

Scaffolds	Porosity (%)	Swelling ratio (%)
CTS	91.94 ± 0.26	97.62 ± 0.34
Lact-CTS-1	92.63 ± 0.42	97.65 ± 0.47
Lact-CTS-2	92.40 ± 0.19	97.83 ± 0.30
Lact-CTS-3	93.44 ± 0.73	98.22 ± 0.25

3.6. Hemolysis Assay. To assess the cytotoxic effect of CTS and Lact-CTS scaffolds on human RBCs, the hemolytic activity of the scaffolds was measured. As illustrated in Figure 8, comparing with negative control, CTS, Lact-CTS-1, and Lact-CTS-2 scaffold extract solutions slightly affected RBCs, whereas Lact-CTS-3 scaffold extract solution caused significant release of hemoglobin from damaged RBCs, probably contributing to a large quantity of Lact-CST-3 dissolved in aqueous solution from the scaffold. This result also suggests that the Lact-CTS-3 scaffold possesses poor stability and biocompatibility.

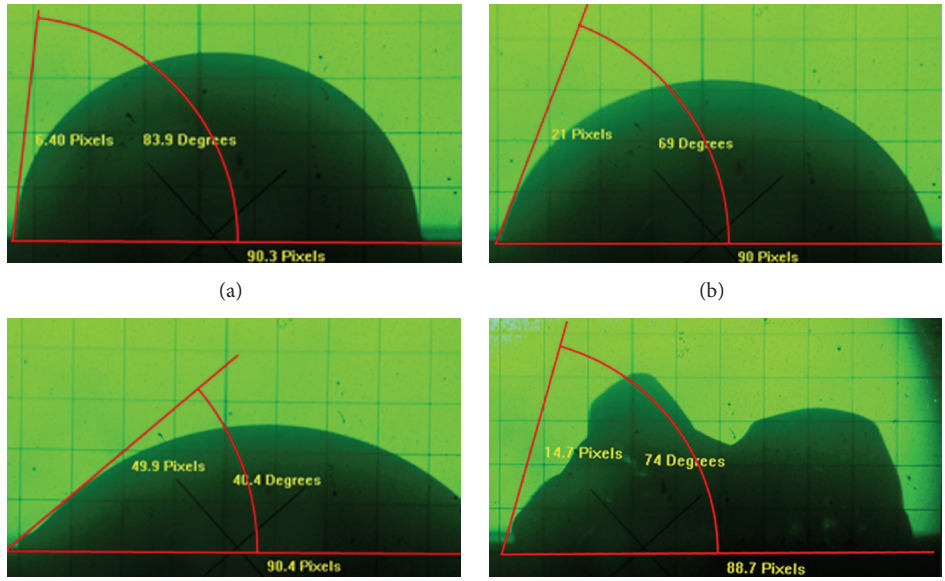

Figure 5: The contact angle of (a) CTS and (b) Lact-CTS-1, (c) Lact-CTS-2, and (d) Lact-CTS-3 measured by the static sessile drop method.

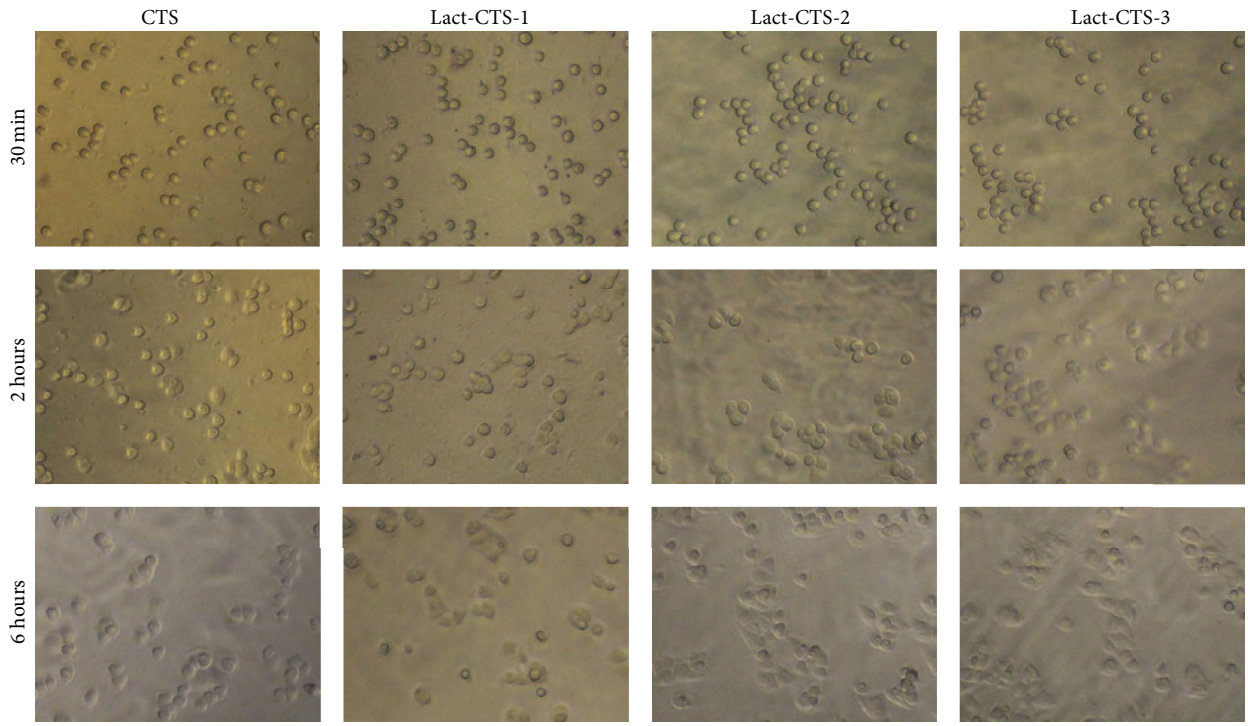

Figure 6: The hepatocytes adhered to CTS, Lact-CTS-1, Lact-CTS-2, and Lact-CTS-3 films under a phase contrast microscope (200x).

4. Conclusions

In this study, the Lact-CTS was successfully synthesized with different DS of galactose moieties through the Schiff base reaction and the reducing action of $NaBH_4$ and then three-dimensional scaffolds were fabricated by freezing-drying technique for liver tissue engineering. The DS of galactose moieties on CTS was 19.66%, 48.62%, and 66.21% in Lact-CTS-1, Lact-CTS-2, and Lact-CTS-3, respectively. The hydrophilicity and cell attachment of Lact-CTS were enhanced along with increasing the galactose moieties, whereas the mechanical stability and biocompatibility were decreased. Therefore, the Lact-CTS-2 scaffold possesses high porosity, better mechanical stability, and excellent

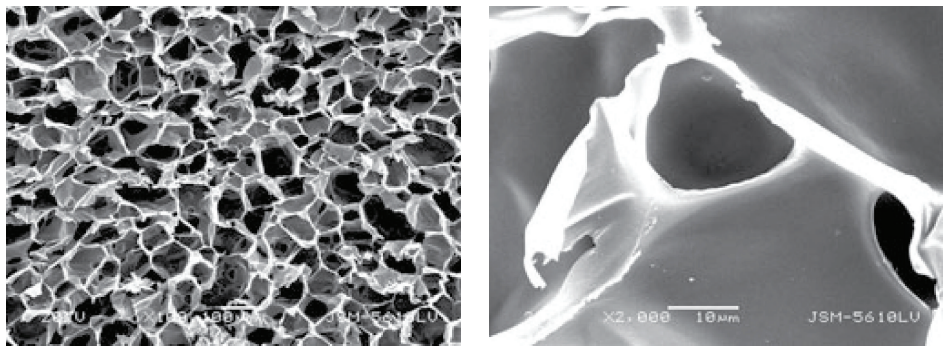

(a) (b)

Figure 7: SEM images of the cross section of Lact-CTS-2 scaffolds.

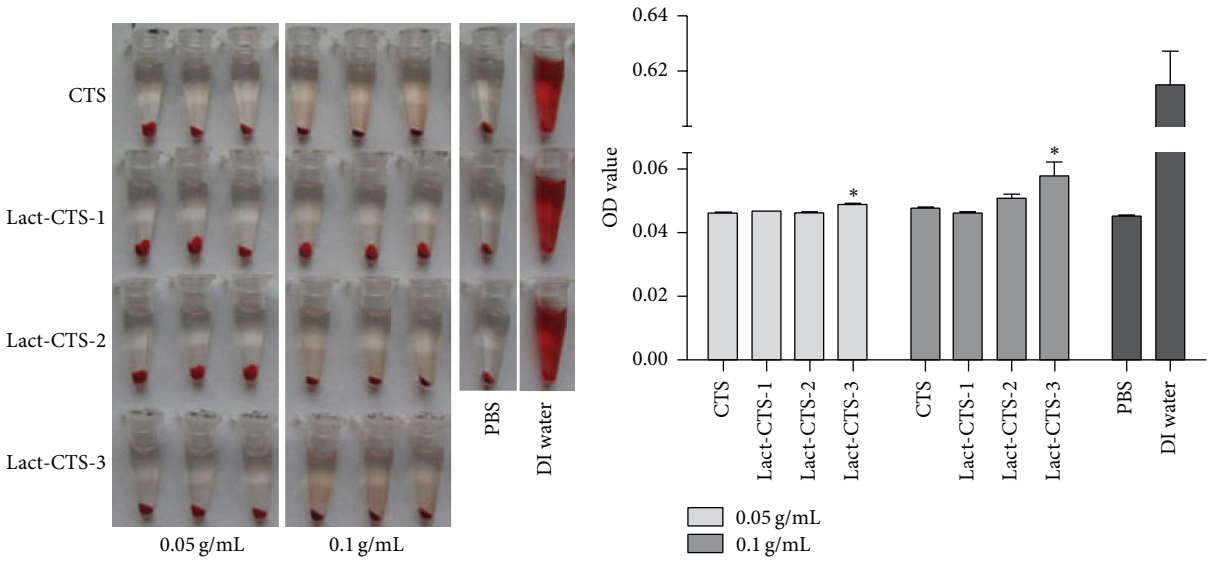

(a) (b)

Figure 8: Hemolysis rate of RBCs treated with CTS, Lact-CTS-1, Lact-CTS-2, and Lact-CTS-3 scaffold extract solutions at concentration of 0.05 and 0.1 g/mL for 3 h. (a) Photographs of hemolysis. (b) Optical density of the supernatant, expressed as means ± SD from three independent experiments and then analyzed by one-way analysis of variance followed by Dunnett's test for comparison against negative control. $^{*}P < 0.05$ compared with negative control group. The presence of hemoglobin in the supernatant indicated damaged RBCs. PBS and DI water were used as the negative and positive controls, respectively.

biocompatibility, indicating that it is a promising material for liver tissue engineering. We are currently working on the maintenance of hepatocellular specific functions on Lact-CTS scaffold in vitro, as well as biodegradation and biocompatibility of scaffolds in vivo.

Conflict of Interests

The authors declare that there is no conflict of interests regarding the publication of this paper.

Authors' Contribution

Birong Wang and Qinggang Hu contributed equally to this work.

Acknowledgments

This work was supported by the Natural Science Foundation of Hubei Province, China (no. 2009CDB275), and partially supported by the National Natural Science Foundation of China (nos. 81372668 and 81502527), Natural Science Foundation of Hubei Province, China (no. 2015CFB527), and Fundamental Research Funds for the Central Universities, China (no. 2014QN064).

References

[1] B.-S. Kim, I.-K. Park, T. Hoshiba et al., "Design of artificial extracellular matrices for tissue engineering," *Progress in Polymer Science*, vol. 36, no. 2, pp. 238–268, 2011.

[2] Z.-Q. Feng, X. Chu, N.-P. Huang et al., "The effect of nanofibrous galactosylated chitosan scaffolds on the formation of rat

primary hepatocyte aggregates and the maintenance of liver function," *Biomaterials*, vol. 30, no. 14, pp. 2753–2763, 2009.

[3] C. S. Cho, S. J. Seo, I. K. Park et al., "Galactose-carrying polymers as extracellular matrices for liver tissue engineering," *Biomaterials*, vol. 27, no. 4, pp. 576–585, 2006.

[4] T. Kean and M. Thanou, "Biodegradation, biodistribution and toxicity of chitosan," *Advanced Drug Delivery Reviews*, vol. 62, no. 1, pp. 3–11, 2010.

[5] M. Tian, B. Han, H. Tan, and C. You, "Preparation and characterization of galactosylated alginate-chitosan oligomer microcapsule for hepatocytes microencapsulation," *Carbohydrate Polymers*, vol. 112, pp. 502–511, 2014.

[6] W. C. Hsieh, J. J. Liau, and Y. L. Li, "Characterization and cell culture of a grafted chitosan scaffold for tissue engineering," *International Journal of Polymer Science*, vol. 2015, Article ID 935305, 7 pages, 2015.

[7] A. Anitha, S. Sowmya, P. T. S. Kumar et al., "Chitin and chitosan in selected biomedical applications," *Progress in Polymer Science*, vol. 39, no. 9, pp. 1644–1667, 2014.

[8] V. Beachley and X. J. Wen, "Polymer nanofibrous structures: fabrication, biofunctionalization, and cell interactions," *Progress in Polymer Science*, vol. 35, no. 7, pp. 868–892, 2010.

[9] I.-K. Park, J. Yang, H.-J. Jeong et al., "Galactosylated chitosan as a synthetic extracellular matrix for hepatocytes attachment," *Biomaterials*, vol. 24, no. 13, pp. 2331–2337, 2003.

[10] J. Fan, Y. Shang, Y. Yuan, and J. Yang, "Preparation and characterization of chitosan/galactosylated hyaluronic acid scaffolds for primary hepatocytes culture," *Journal of Materials Science: Materials in Medicine*, vol. 21, no. 1, pp. 319–327, 2010.

[11] F. Chen, M. Tian, D. Zhang et al., "Preparation and characterization of oxidized alginate covalently cross-linked galactosylated chitosan scaffold for liver tissue engineering," *Materials Science and Engineering C*, vol. 32, no. 2, pp. 310–320, 2012.

[12] M. Li, Y. Hong, Z. Wang et al., "Fabrication of chitosan nanoparticles with aggregation-induced emission characteristics and their applications in long-term live cell imaging," *Macromolecular Rapid Communications*, vol. 34, no. 9, pp. 767–771, 2013.

[13] H. Chen, M. Li, T. Wan et al., "Design and synthesis of dual-ligand modified chitosan as a liver targeting vector," *Journal of Materials Science: Materials in Medicine*, vol. 23, no. 2, pp. 431–441, 2012.

[14] Z. Wang, S. Chen, J. W. Y. Lam et al., "Long-term fluorescent cellular tracing by the aggregates of AIE bioconjugates," *Journal of the American Chemical Society*, vol. 135, no. 22, pp. 8238–8245, 2013.

[15] Y. Chen, Y. Ye, Y. Jing, Y. Gao, Y. Guo, and H. Tan, "The synthesis of the locating substitution derivatives of chitosan by click reaction at the 6-position of chitin," *International Journal of Polymer Science*, vol. 2015, Article ID 419506, 9 pages, 2015.

[16] P. H. Weigel, "Rat hepatocytes bind to synthetic galactoside surfaces via a patch of asialoglycoprotein receptors," *The Journal of Cell Biology*, vol. 87, no. 3, pp. 855–861, 1980.

[17] W. Xu, L. Cao, L. Chen et al., "Isolation of circulating tumor cells in patients with hepatocellular carcinoma using a novel cell separation strategy," *Clinical Cancer Research*, vol. 17, no. 11, pp. 3783–3793, 2011.

[18] I. Donati, S. Stredanska, G. Silvestrini et al., "The aggregation of pig articular chondrocyte and synthesis of extracellular matrix by a lactose-modified chitosan," *Biomaterials*, vol. 26, no. 9, pp. 987–998, 2005.

[19] X. P. Kong, "Simultaneous determination of degree of deacetylation, degree of substitution and distribution fraction of -COONa in carboxymethyl chitosan by potentiometric titration," *Carbohydrate Polymers*, vol. 88, no. 1, pp. 336–341, 2012.

[20] G. Luna-Barcenas, D. G. Zarate-Triviño, Z. García-Carvajal et al., "Mammalian cell culture on a novel chitosan-based biomaterial crosslinked with gluteraldehyde," *Macromolecular Symposia*, vol. 283-284, no. 1, pp. 181–190, 2009.

[21] J. Huang, L. Zhang, B. Chu, X. Peng, and S. Tang, "Repair of bone defect in caprine tibia using a laminated scaffold with bone marrow stromal cells loaded poly (L-lactic acid)/β-tricalcium phosphate," *Artificial Organs*, vol. 35, no. 1, pp. 49–57, 2011.

[22] R. Zhang and P. X. Ma, "Poly(α-hydroxyl acids)/hydroxyapatite porous composites for bone-tissue engineering. I. Preparation and morphology," *Journal of Biomedical Materials Research*, vol. 44, no. 4, pp. 446–455, 1999.

[23] Y.-S. Lin and C. L. Haynes, "Impacts of mesoporous silica nanoparticle size, pore ordering, and pore integrity on hemolytic activity," *Journal of the American Chemical Society*, vol. 132, no. 13, pp. 4834–4842, 2010.

[24] C. Li, D. Zhong, Y. Zhang et al., "The effect of the gene carrier material polyethyleneimine on the structure and function of human red blood cells in vitro," *Journal of Materials Chemistry B*, vol. 1, no. 14, pp. 1885–1893, 2013.

[25] G. Altankov, V. Thom, T. Groth, K. Jankova, G. Jonsson, and M. Ulbricht, "Modulating the biocompatibility of polymer surfaces with poly(ethylene glycol): effect of fibronectin," *Journal of Biomedical Materials Research*, vol. 52, no. 1, pp. 219–230, 2000.

[26] S.-J. Seo, T. Akaike, Y.-J. Choi, M. Shirakawa, I.-K. Kang, and C.-S. Cho, "Alginate microcapsules prepared with xyloglucan as a synthetic extracellular matrix for hepatocyte attachment," *Biomaterials*, vol. 26, no. 17, pp. 3607–3615, 2005.

[27] M. Li, J. W. Y. Lam, F. Mahtab et al., "Biotin-decorated fluorescent silica nanoparticles with aggregation-induced emission characteristics: fabrication, cytotoxicity and biological applications," *Journal of Materials Chemistry B*, vol. 1, no. 5, pp. 676–684, 2013.

[28] F. Zhao, Y. Zhao, Y. Liu, X. Chang, C. Chen, and Y. Zhao, "Cellular uptake, intracellular trafficking, and cytotoxicity of nanomaterials," *Small*, vol. 7, no. 10, pp. 1322–1337, 2011.

[29] C. S. Ranucci and P. V. Moghe, "Polymer substrate topography actively regulates the multicellular organization and liver-specific functions of cultured hepatocytes," *Tissue Engineering*, vol. 5, no. 5, pp. 407–420, 1999.

[30] J. Hodde, A. Janis, and M. Hiles, "Effects of sterilization on an extracellular matrix scaffold: part II. Bioactivity and matrix interaction," *Journal of Materials Science: Materials in Medicine*, vol. 18, no. 4, pp. 545–550, 2007.